

# The effect of laser texturing of SiC surface on the critical load for the transition of water lubrication mode from hydrodynamic to mixed

Xiaolei Wang <sup>a,\*</sup>, Koji Kato <sup>a</sup>, Koshi Adachi <sup>a</sup>, Kohji Aizawa <sup>b</sup>

<sup>a</sup> *Laboratory of Tribology, School of Mechanical Engineering, Tohoku University, Sendai 980-8579, Japan*

<sup>b</sup> *Mechanical Engineering Research Laboratory, Hitachi Ltd, 502 Kandatsu, Tsuchiura, Ibaraki 300-0013, Japan*

Received 13 July 2000; accepted 7 June 2001

## Abstract

Experiments were carried out to verify if the low friction range of SiC in water lubrication can be expanded by micro-pores on the contact surface. Pores were formed by laser, with a diameter of 150  $\mu\text{m}$  and a depth of about 8–10  $\mu\text{m}$  and were distributed in a square array on the contact surface. Seven kinds of textured specimens with different intervals between the pores were tested and compared with the untextured specimen. The effect of the pore area ratio on friction coefficient and the critical load for the transition from hydrodynamic lubrication to mixed lubrication was reported and discussed. © 2001 Elsevier Science Ltd. All rights reserved.

*Keywords:* Pore; SiC; Water lubrication; Lubrication mode; Transition

## 1. Introduction

Fine ceramics are being used for tribo-elements due to their excellent physical, chemical and mechanical properties such as low density, low thermal expansion, good corrosion resistance and high hardness over a wide range of temperatures, etc. In particular, a very low friction coefficient ( $<0.002$  for  $\text{Si}_3\text{N}_4$  [1], 0.0038 for SiC [2]) was observed in water lubrication for the ceramics of the Si family. The reason for this is that the tribochemical reaction product  $\text{SiO}_2$  and its hydride are dissolved in water in the form of silicic acid which is recognized to act as a lubricant, and the contact surfaces become very smooth due to tribochemical wear [1–5]. Comparing the two main types of Si ceramics, silicon carbide (SiC) maintains low friction in a much wider speed range, although its minimum friction coefficient is not as low as that of silicon nitride. In addition, SiC has better anti-seizure, anti-wear and heat conduction properties. As a result, SiC has become a notable

material for mechanical seals and sliding bearings of hydraulic machines in recent years [6,7].

The problem of seizure, however, still remains in some particular situations for bearings and seals. Furthermore, along with the development of industry, more and more machine components which can work in severe conditions are needed.

The study of the hydrodynamic effect of surface texture has a long history. It was found that a certain type of micro-texture is effective for generating additional load capacity or separating force between parallel sliding faces. The key point of this phenomenon is cavitation. Generally, the pressure increases in the converging film regions, while it decreases in the diverging film regions for incompressible fluids. The cavity generated in diverging film regions is, theoretically, an isobaric region. The pressure in this region cannot be lower than the cavity pressure, which is the fluid vapor pressure or the pressure at which the lubricant is saturated with the gas dissolved in it. As a result, the pressure increase in the converging film regions can be much larger than the pressure drop in the diverging film regions. So, additional load capacity or separate force is generated by texture between contact surfaces [8–12].

\* Corresponding author.

*E-mail address:* xlwang@tribo.mech.tohoku.ac.jp (X. Wang).

Another lubrication effect of texture on the intimate contact surface is the so-called secondary lubrication mechanism. In other words, the liquid trapped in the low region of the texture can be considered as a secondary source of lubricant that permeates to the surface to reduce the friction and retard the galling during sliding [13,14].

However, it is still difficult for an analytical experiment to yield true and exact results for the case of texture lubrication, although it is recognized as a useful method to obtain certain trends of the influence of surface texture from a variety of parameters. Particularly for the ceramics of the Si family, so little is known about the properties of tribochemical products that it is very difficult to simulate the lubrication condition even without surface texture. Comparatively, an analytical experiment is a realizable method that is able to give comprehensive results of the effect of a certain texture pattern.

It was proved that lasers are an efficient and controllable method for producing the texture of micro-pores [15,16]. Halperin and colleagues performed an experiment on a laser-textured seal ring of steel with micro-pores of various depths to demonstrate the potential of the surface texturing technology. It was found that optimized spherical pores can maximize the film stiffness and the PV factor at seizure inception over an untextured ring by at least 150% in oil lubrication [17]. Results of an analytical solution indicate that the effect of the pore depth on the diameter ratio is more significant than that of the area density (or area ratio) of the pores [18].

Tejima et al. formed micro-pores on the surface of SiC by way of micro-blast, and carried out friction experiments between the faces of carbon and SiC under water lubrication. It was confirmed that the minimum friction coefficient could be reduced by pores with an optimized diameter [19,20].

In these situations of water lubrication of SiC and the surface texturing effect on lubrication, the purpose of this study is to ascertain the effect of texturing of the SiC surface on the critical load for the transition of water lubrication mode from hydrodynamic to mixed. Fine pores were formed on the SiC disk by laser texturing for this purpose, and experiments were carried out.

## 2. Experimental details

### 2.1. Specimens

The sliding friction experiments were performed between the end faces of a disk (Fig. 1(a)) and a cylinder (Fig. 1(b)) under water lubrication. Both disk and cylinder were made of SiC, and the end faces were ground to the roughness of  $R_{rms}$  to around 200 nm.

The end face of the disk was textured to the pattern shown in Fig. 2 by a CO<sub>2</sub> laser. The diameter and depth

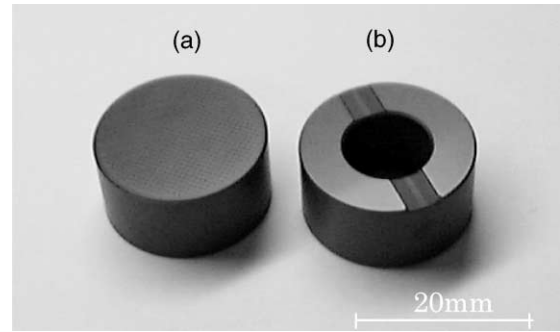


Fig. 1. Appearance of specimens: (a) disk, and (b) cylinder.

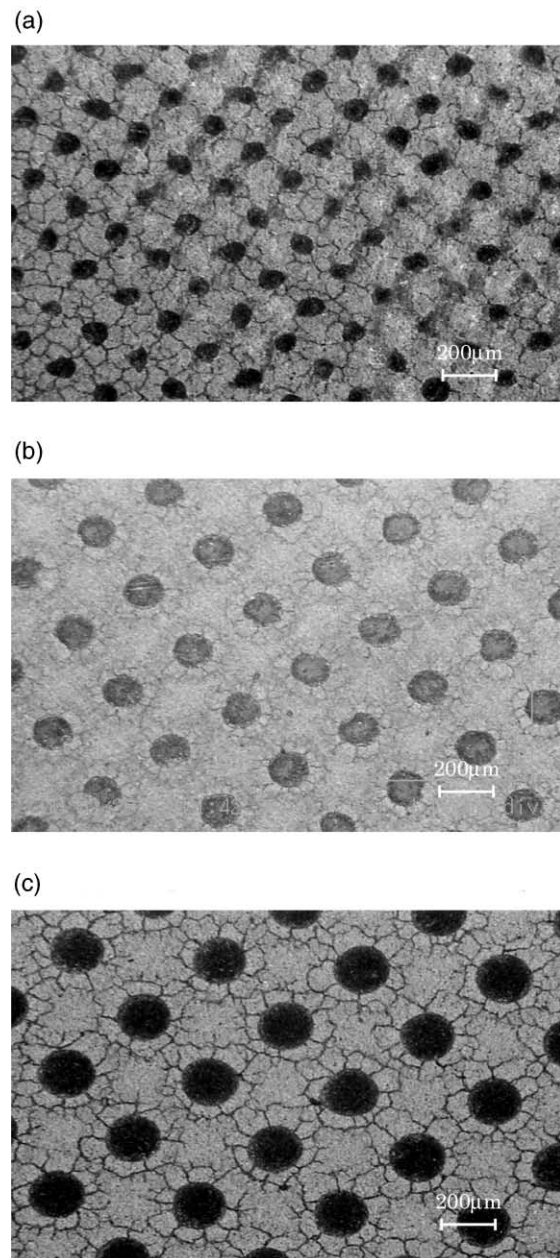


Fig. 2. Optical micrographs of pores on the disk surface produced by laser texturing. (a) The pores with diameter of 100  $\mu\text{m}$ ; (b) the pores with diameter of 150  $\mu\text{m}$ ; (c) the pores with diameter of 200  $\mu\text{m}$ .

of the pores were determined according to the power and pulse width of the laser. The interval between pores was changed to get a series of pore area ratios.

$$r = \frac{S_p}{S} = \frac{\pi d^2}{4l^2} (\%)$$

where  $r$  is the pore area ratio,  $S_p$  is the area occupied by pores,  $S$  is the area of the end surface of the disk,  $d$  is the pore diameter and  $l$  is the interval between pores.

After laser treatment, the disk was ground again to remove the bulges on the pore rims formed by the heat, and to make the area beside the pores of the same roughness as that of the end surface of the cylinder.

All cylinders (Fig. 1(b)) were the same with a hole in the center and two grooves on the contact surface so that lubricant was supplied from the center to the friction surface.

It was also planned to investigate the effect of the diameter of the pores. Figs. 2(a)–(c) show pores of diameter 100, 150, and 200  $\mu\text{m}$ . In the case of a 100  $\mu\text{m}$  diameter, it seems that the laser was not powerful enough to vapor or melt the anisotropic material evenly so that symmetrical round pores could not be generated. In contrast, in the case of a 200  $\mu\text{m}$  diameter, the laser was too powerful, so that a lot of cracks were formed around the pores. Hence, only the specimens with pores of 150  $\mu\text{m}$  were finally tested. However, even in these pores there was a ring-like heat affected area around the pores, where there were some small cracks (Fig. 3). The results of the Vickers test showed that the hardness of this area (about 2000) was somewhat lower than that of the original surface (about 2600), so, after grinding, the height of this area seemed lower than the remaining area. The profile scan results show that the difference of the surface height is about 10–30 nm.

The geometrical parameters of the specimens used in this study are shown in Table 1. The pore area ratios are in the range of 0–22.5%.

## 2.2. Test set

Fig. 4 shows the apparatus used in this experiment. The cylinder was driven by a motor to a certain rotational speed which could be adjusted in the range of 200–1500 rpm. Load was applied by a hydraulic system via the bottom of the disk. Purified water was supplied by a volume controllable pump to the center of the cylinder via the grooves and then to the contact surfaces. Water was used only once to avoid the influence of wear products. The temperature of the lubricant when it flowed in and out of the friction pair was monitored by a thermocouple. Load and friction torque were detected by load cells. Air bearing was used to support the disk so that a very small friction torque ( $<0.001$  Nm) could be detected accurately.

The testing conditions are shown in Table 2.

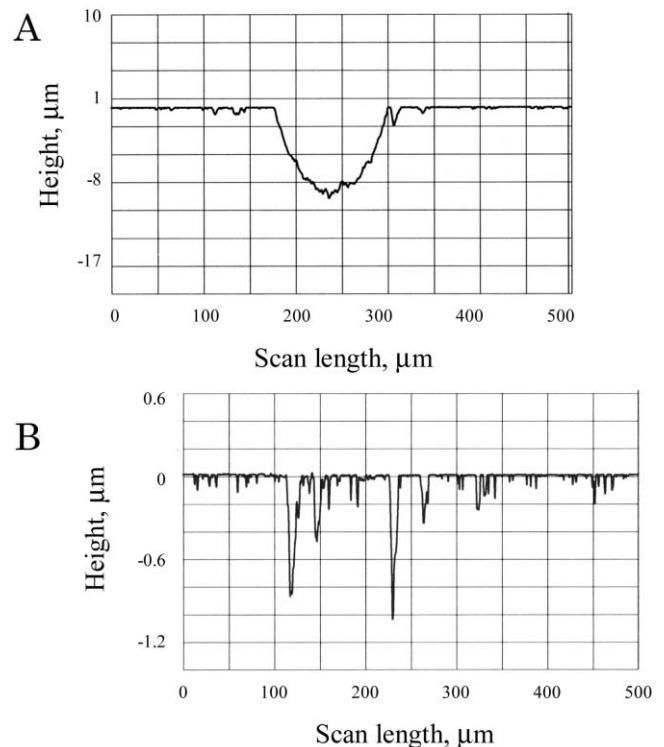
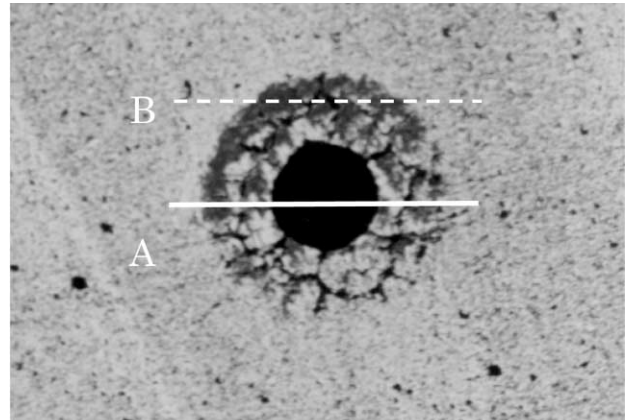


Fig. 3. Profiles of the pore of diameter 150  $\mu\text{m}$  and the heat affected zone: (A) at the pore center, and (B) at the heat affected zone.

## 2.3. Test procedure

Previous works have shown that surface roughness plays an important role in the friction and lubrication of SiC since the thickness of the lubrication film is estimated to be around 1  $\mu\text{m}$  [5]. In addition, inappropriate polishing often causes the problem of flatness degradation which is also very important for the generation of lubrication film. So all the specimens had the same running-in procedure before measurement. Fig. 5 shows the detailed procedure of running-in, which was performed at a rotational speed of 1000 rpm, and the friction properties of SiC during running-in. When the load was raised, the friction torque jumped to a high level and then decreased. This implies that the contact and the

Table 1  
Geometrical parameters of texture on the disk surface<sup>a</sup>

No.	Pore diameter $d$ ( $\mu\text{m}$ )	Pore depth $h$ ( $\mu\text{m}$ )	Pore interval $l$ ( $\mu\text{m}$ )	Pore area ratio $r$ (%)
1	0	0	0	0
2	150	8~11	800	2.8
3	150	8~11	600	4.9
4	150	8~11	500	7
5	150	8~11	450	8.7
6	150	8~11	400	11
7	150	8~11	350	14.4
8	150	8~11	280	22.5

<sup>a</sup> Disk end surface area=314.2 mm<sup>2</sup>.

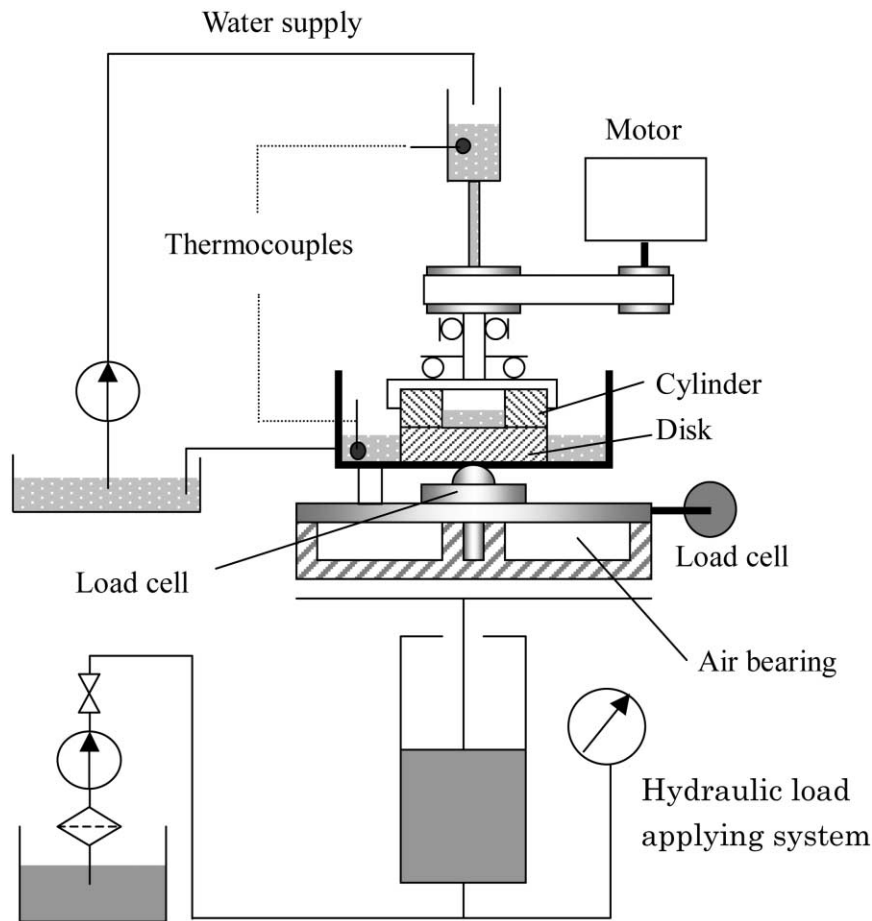


Fig. 4. Schematic diagram of the experimental apparatus.

Table 2  
Experimental conditions

Load	98~2548 N
Rotational speed	200~1200 rpm
Lubricant	Purified water
Supply rate	60 ml/min
Room temperature	15~18°C
Humidity	30~40%

lubrication conditions were improved by wear. Furthermore, the rate of friction torque decrease could be regarded as the running-in rate. So after friction torque no longer decreased, a higher load was applied. This step was repeated in increments of about 100 N until the friction torque no longer decreased and reached the upper limit of the load cell (experience has shown that if the load is increased continually, seizure will occur between the contact surfaces). After the procedure of running-in, the surface around the pores was worn and became

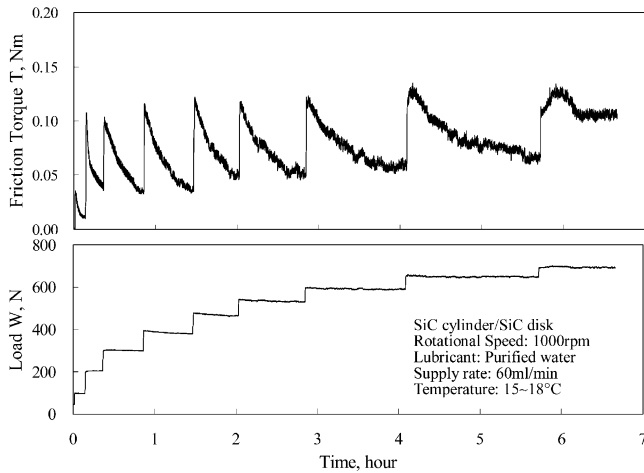


Fig. 5. Typical running-in procedure.

smooth. Then the friction tests under various loads and speeds were performed. The friction coefficient was calculated as follows:

$$\mu = \frac{T}{WR}$$

where  $\mu$  is the friction coefficient,  $T$  is the friction torque,  $W$  is the load and  $R$  is the average radius of the contact area.

#### 2.4. Results

Typical trends of friction coefficient under different loads and speed conditions are summarized in Fig. 6 (SiC cylinder/untextured SiC disk) and Fig. 7 (SiC cylinder/textured SiC disk). These figures show that the friction coefficient stays at a very low level while the load is light, but after the load exceeds a certain value, the friction suddenly rises. If the load is increased continually seizure occurs, although the value of the friction

coefficient is not very high ( $<0.01$ ) at that time. The next point to be noted is that this “certain value of load” increases when rotational speed is raised.

The experimental results of the disks with different pore area ratios are presented in Fig. 8. It is obvious that friction properties are influenced by the pore area ratio, and the low friction region of SiC sliding in water can be expanded by micro-pores with a certain value of pore area ratio.

Fig. 9 shows the typical Stribeck curve of self-mated SiC sliding in water. First, it is interesting to note that the data obtained from different rotational speeds cannot be unified into one Stribeck curve. That means, the Sommerfeld value, which divides the lubrication mode, changes according to the change in rotational speed, thus confirming that the friction of SiC under water lubrication is different to that of metal in oil. This supports the view that the film thickness is not a linear function of speed, or the lubricant has properties different to Newtonian fluid. The value of the friction coefficient in the low-friction region is very small, approximately 0.001–0.003, suggesting that it is in a state of hydrodynamic lubrication. So the sudden increase in the friction coefficient from a stable low value should be considered as the transition of the lubrication mode from hydrodynamic to mixed and above.

Therefore, the load which causes the sudden increase in the friction coefficient (Figs. 6 and 7) is defined as the critical load ( $W_c$ ) for the transition of the lubrication mode. It is used to evaluate the effect of surface texture in this experiment. High critical load means the hydrodynamic lubrication region is wide and the load carrying capacity is high.

Fig. 10 shows the effect of pore area ratio on the critical load  $W_c$  at rotational speeds of 400, 800 and 1200 rpm. It is clear that within the pore area ratio range of 0–10%, the critical load for the transition can be

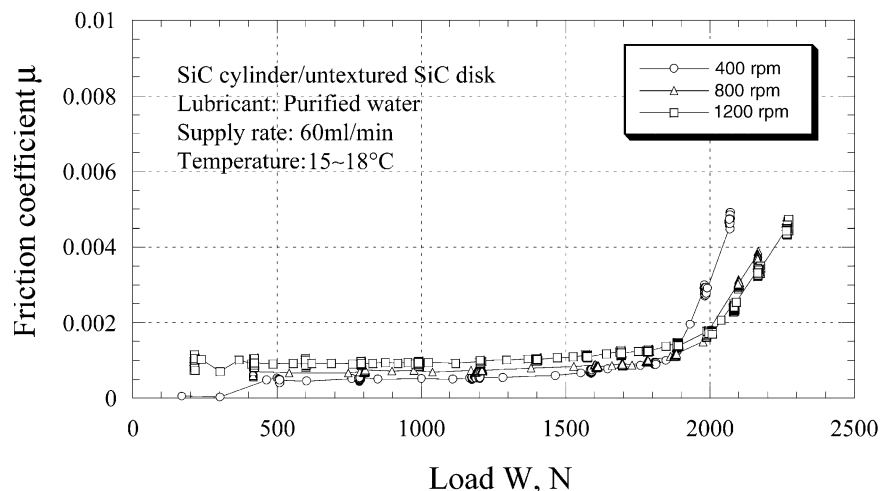


Fig. 6. Friction coefficient  $\mu$  versus load  $W$  for a SiC cylinder/untextured SiC disk in water at three different rotational speeds.

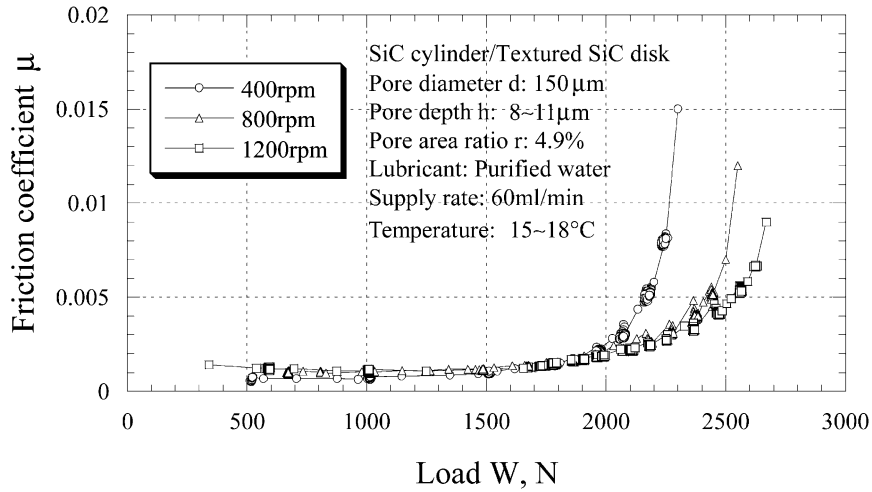


Fig. 7. Friction coefficient  $\mu$  versus load  $W$  for a SiC cylinder/SiC textured disk in water at three different rotational speeds.

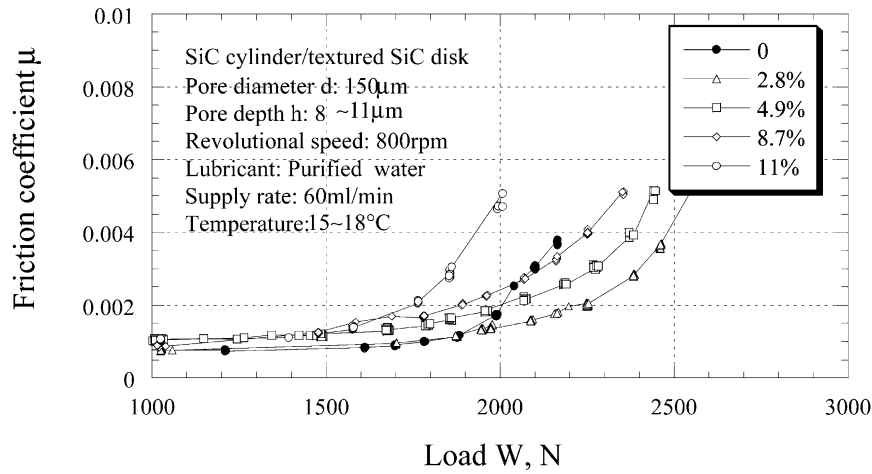


Fig. 8. Friction coefficient  $\mu$  versus load  $W$  for a SiC cylinder/SiC disk in water with different pore area ratios.

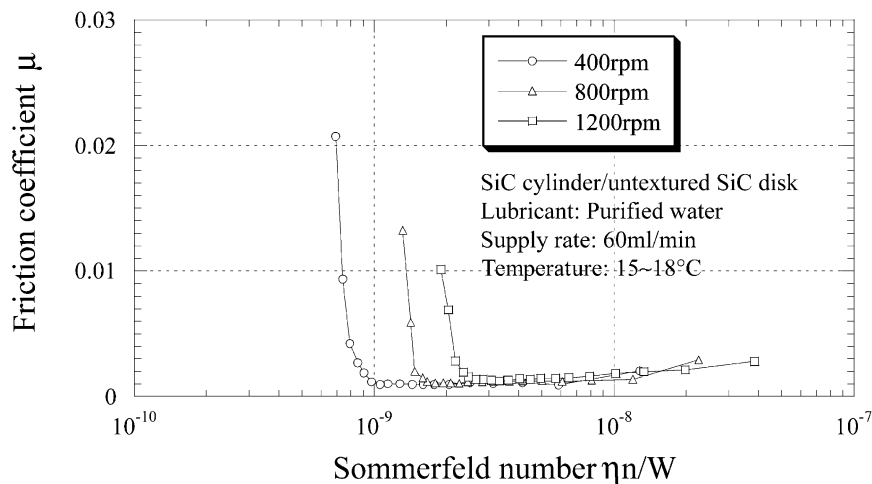


Fig. 9. Stribeck curves for a SiC cylinder/SiC untextured disk in water.

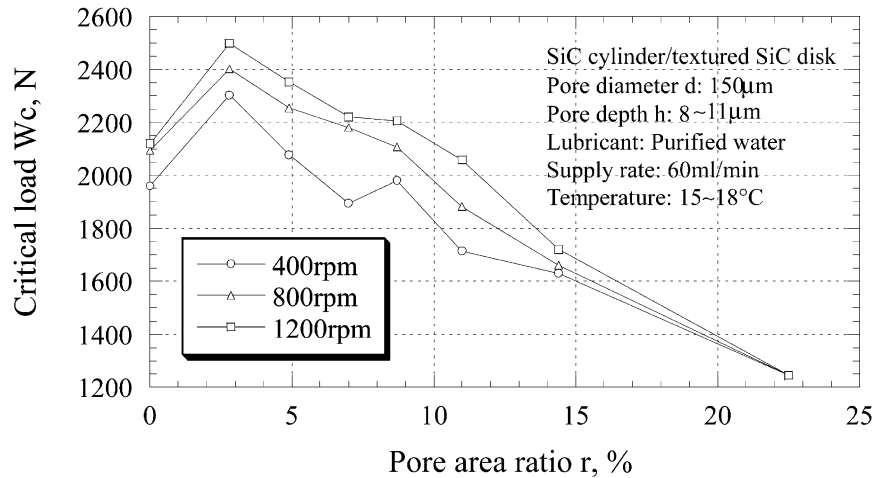


Fig. 10. The effect of pore area ratio on the critical load for the transition from mixed lubrication to hydrodynamic lubrication of a SiC cylinder/SiC textured disk in water.

increased by surface texture. Furthermore, the disk with the pore area ratio of 2.8% in this experiment gave the best result of a near 20% increase in the critical load compared with the untextured specimen. When the pore area ratio exceeded 10%, the critical load  $W_c$  decreased to a value lower than that of the untextured specimen, therefore, it did not provide any improvement to the load carrying capacity.

Fig. 11 shows the range of pore area ratio and rotational speed in which the critical load  $W_c$  was increased or decreased. The conditions marked “○” are those at which the critical load was increased, and “●” means the critical load was decreased at that condition. It is clear that three regions exist in this figure. In region I, the critical load  $W_c$  is increased within the whole speed range, whereas region III is the opposite. In region II, the critical load is only increased at high rotational speed.

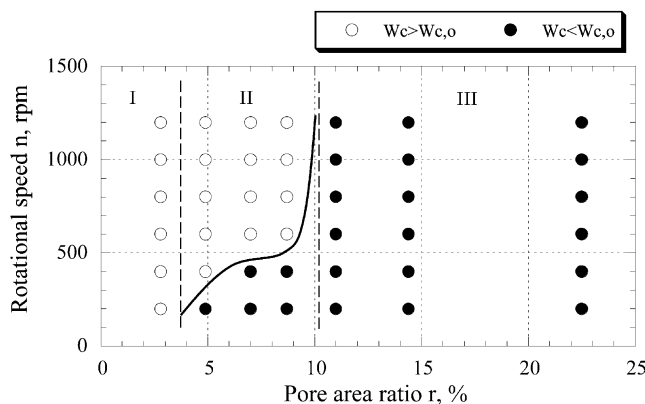


Fig. 11. Rotational speed and pore area ratio range for an increase/decrease in critical load.  $W_c$ , critical load for the transition from hydrodynamic lubrication to mixed lubrication;  $W_{c,0}$ , critical load of the specimen without texture (pore area ratio  $r=0\%$ ).

## 2.5. Discussion

The texture on the contact surface of SiC improves the performance of lubrication. At the same time, it reduces the load supporting area and leads to an increase in the surface contact pressure. Although the pore area ratios of the specimens used in this experiment were not very high, Fig. 3 shows that the diameter of the heat affected area was as large as 300–450  $\mu\text{m}$  for the pore of  $\phi 150 \mu\text{m}$ . This means that the heat unaffected area was extremely small for specimens with a pore area ratio larger than 10% (Table 3). The most obvious effects of heat are those already mentioned, that is, the generation of cracks and a decrease in hardness. These effects prevented the surface from becoming as smooth as the original surface after running-in. This is a necessary condition so that the contact surfaces of SiC maintain a low-friction condition since the lubrication film was estimated to be very thin. Furthermore, the decrease in hardness resulted in the properties of the material changing with heat. This also implies that it was possible that the performance of the tribochemical reaction was also changed by heat.

Another interesting point is the shape of the pore cross section (Fig. 3). If the main advantage of the texture comes from the hydrodynamic effect, then a laser is better than other methods such as etching which usually makes the walls of the pores near vertical to the friction surface. However, if low friction is due to the lubricant stored in the pores, which helps to generate the product of the tribochemical reaction, different shapes of cross section may result in the same effect.

Fig. 12 shows the effect of rotational speed on the critical load for untextured and textured specimens with three different pore area ratios. It is clear that there is a linear dependence of the critical load on the rotational

Table 3  
Heat affected area<sup>a</sup>

No.	Pore diameter $d$ ( $\mu\text{m}$ )	Pore area ratio $r$ (%)	Diameter of heat affected area $d_h$ ( $\mu\text{m}$ )	Area ratio of heat affected area $r_h$ (%)
1	0	0	0	0
2	150	2.8	300~450	11~24.8
3	150	4.9	300~450	19.6~44.2
4	150	7	300~450	28.3~63.6
5	150	8.7	300~450	34.9~78.5
6	150	11	300~450	44.2~99.4
7	150	14.4	300~450	57.7~100
8	150	22.5	300~450	90.2~100

<sup>a</sup> Disk end surface area=314.2 mm<sup>2</sup>.

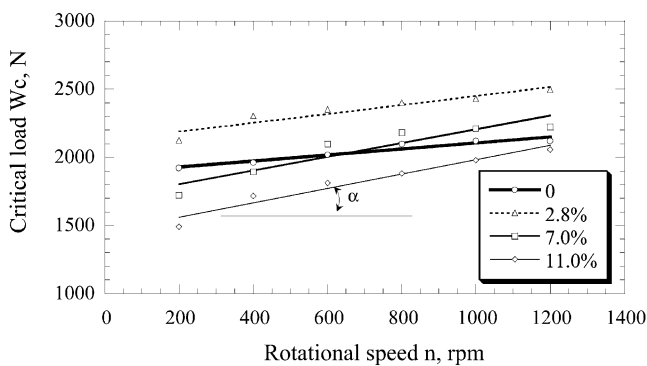


Fig. 12. Linear dependence of critical load on rotational speed for untextured and textured (with three different pore area ratios) SiC sliding in water.

speed for both untextured and textured specimens. Mathematically, compared with the untextured specimen, the slope  $\alpha$  and the interception of the lines are changed by surface texturing. The fact that the slope of the lines is increased by the texture implies hydrodynamic lubrication occurs more readily with the textured specimen than with the untextured specimen. The reason why the interceptions of the lines with the pore area ratios of 7 and 11% decrease may be due to the increase in the contact pressure. However, for a low pore area ratio, such as 2.8% in this graph, the contact pressure does not increase sufficiently so that the storage effect of the lubricant in the pores becomes dominant, raising the interception of this line.

### 3. Conclusion

In order to increase the load carrying capacity of a SiC cylinder sliding on a SiC disk in water with the mode of hydrodynamic lubrication, fine pores were introduced on the disk surface by laser texturing. The pore effect on the critical load for the transition from hydrodynamic to mixed lubrication was then studied experimentally.

It is concluded that there exists an optimum value of pore area ratio to give the largest value of critical load. In this study it was 2.8% for SiC and the critical load was larger than that of the untextured surface by 20%. This effect was maintained in the speed range between 400 and 1200 rpm.

### References

- [1] Tomizawa H, Fischer TE. Friction and wear of silicon nitride and silicon carbide in water: hydrodynamic lubrication at low sliding speed obtained by tribochemical wear. *ASLE Trans* 1987;30(1):41–6.
- [2] Wong HC, Umehara N, Kato K. Frictional characteristics of ceramics under water-lubricated conditions. *Tribol Lett* 1998;5(4):303–8.
- [3] Sugita T, Ueda K, Kanemura Y. Material removal mechanism of silicon nitride during rubbing in water. *Wear* 1984;97:1–8.
- [4] Ishigaki H, Nagata R, Iwasa M. Effect of absorbed water on friction of hot-pressed silicon nitride and silicon carbide at low speed sliding. *Wear* 1988;121:107–16.
- [5] Wong HC, Umehara N, Kato K. The effect of surface roughness on friction of ceramics sliding in water. *Wear* 1998;218(2):237–43.
- [6] Enomoto Y. Present and future technology for ceramics. *J Jap Soc Tribologists* 1992;37(9):722–7.
- [7] Nau BS. Mechanical seal face materials. *Proc Instn Mech Engrs* 1997;211(J):165–83.
- [8] Hamilton DB, Walowit JA, Allen CM. A theory of lubrication by micro-irregularities. *Trans ASME, J Basic Eng* 1966;88(1):177–85.
- [9] Findlay JA. Cavitation in mechanical face seals. *Trans ASME, J Lubrication Technol* 1968;April:356–64.
- [10] Anno JN, Walowit JA, Allen CM. Load support and leakage from microasperity-lubricated face seals. *Trans ASME, J Lubrication Technol* 1969;October:726–31.
- [11] Lai T, Grove M. Development of non-contacting, non-leaking spiral groove liquid face seals. *Lubrication Eng* 1994;8:625–31.
- [12] Etsion I, Burstein L. A model for mechanical seals with regular micro surface structure. *Tribol Trans* 1996;139(3):677–83.
- [13] Lo SW, Horng TC. Lubricant permeation from micro oil pits under intimate contact condition. *Trans ASME, J Tribol* 1999;121:633–8.
- [14] Lo SW, Wilson WRD. A theoretical model of micro-pool lubrication in metal forming. *Trans ASME, J Tribol* 1999;121:731–8.
- [15] Baumgart P, Krajnovich DJ, Nguyen TA, Tam AC. A new laser



- texturing technique for high performance magnetic disk drives. *IEEE Trans Magn* 1995;31(6):2946–51.
- [16] Geiger M, Roth S, Becker W. Influence of laser-produced microstructures on the tribological behaviour of ceramics. *Surf Coat Technol* 1998;101(1-3):17–22.
- [17] Halperin G, Greenberg Y, Etsion I. Increasing mechanical seal life with laser-textured seal faces. In: *Proceedings of the 15th International Conference on Fluid Sealing*. Maastricht: BHR Group, 1997:3–11.
- [18] Etsion I, Kligerman Y. Analytical and experimental investigation of laser-textured mechanical seal faces. *STLE Tribol Trans* 1999;42(3):511–6.
- [19] Tejima Y, Ishiyama S, Ura A. The influence of pores at sliding faces and the pores diameter on mechanical seals performance. *J Jap Soc Tribologists* 1999;44(6):54–61.
- [20] Tejima Y, Ishiyama S, Ura A. The influence of rounded pore's diameter and depth at sliding faces for coefficient of friction under oil lubrication. *J Jap Soc Tribologists* 1999;44(10):64–71.